Candle Flame Simulation Considering Temperature Change in the Environment

Nobuhiko Mukai[1,2][a], Reina Arai[1] and Youngha Chang[1]

[1]*Knowledge Engineering, Tokyo City University, 1-28-1 Tamazutsumi, Setagaya, Tokyo 158-8557, Japan*
[2]*Institute of Industrial Science, The University of Tokyo, 4-6-1 Komaba, Meguro, Tokyo, 153-8505, Japan*

Keywords: Fluid Dynamic Simulation, Particle Method, SPH, Candle Flame.

Abstract: Fire simulations are utilized in many scenes such as explosion and conflagration in movies or games, and a lot of techniques have been developed. Some are used to control the flame shape for animations, and others are for real and real-time visualizations. In fact, the flame color changes according to the combustion states: complete combustion, incomplete combustion, and non-combustion. Almost all previous studies, however, performed flame simulations considering only one state of incomplete combustion. Then, we have been researching the candle flame visualization considering three combustion states, and the color changed depending on the combustion state. However, the candle flame length was too short in the previous method. Therefore, we propose a method to consider the temperature change that affects the air density in the environment. The change of the environmental air density induces the external force, which makes the shape of the candle flame. As the result of the simulation, the candle flame shape has become thinner than before and has been similar to that of a real candle flame.

1 INTRODUCTION AND RELATED WORKS

It is said that human is the only animal who can treat fire, and this specific character differentiates human beings from other animals. Fire is very familiar to us and important in our daily life. In TV dramas, movies, and games, there are many scenes where the fire appears such as explosions and conflagrations; however, fire is also dangerous so careful attention should be paid when it is treated. Then, some scenes are generated by using computer graphics instead of real videos; however, it is difficult to create realistic movies by controlling the flame because the shape changes dynamically according to the environment such as wind, obstacles, and flammable materials.

With these backgrounds, there are many kinds of previous research related to fire. For example, (Louchez et al., 2006) proposed a model to simulate and represent a candle flame by solving the Navier-Stokes equations with a particle method, and decided the shape as the NURBS (Non-Uniform Rational B-Spline) surface that is defined with particle positions. The flame shape was physically correct; how-

_____

[a] https://orcid.org/0000-0001-8909-9454

ever, artists could not control the shape of the fire. Then, (Bangalore and House, 2012) enabled artists to draw fire paintings freely. Their approach was based on the physical simulation; however, the individual flames were drawn along the curve that artists specified by controlling the direction of the gravity and the buoyancy. (Sato et al., 2017) also proposed a feedback control method for users to design a fire shape with control points. Their method employed a PID (Proportional Integral Derivative) controller to adjust the force and the temperature. In addition, (Hladký, 2018) proposed a system, with which users could control the fire. Their method extended the Navier-Stokes equations by considering the wind field, the diffusion, the source motion, and the buoyancy terms, and the in-between images were generated based on the hand-drawn keyframes.

On the other hand, there are some particle-based researches related to the simulations and the rendering techniques of fire since it requires a lot of particles and computational resources to simulate and visualize the flame of fire. (Wei et al., 2002) employed the LBM (Lattice Boltzmann Model) for physically-based simulation, and used textured splats for the rendering. (Horvath and Geiger, 2009) also proposed a GPU-based volume rendering method. Their method used

_____

the combination of the coarse particle grid simulation, and the fine and view-oriented refinement simulation. In the method, the multiple independent GPUs refined the final simulation for the rendering. In addition, (Cha et al., 2009) used pre-calculated CFD (Computational Fluid Dynamics) data to generate the fire scene and developed a firefighter training simulator. On the other hand, (Guay et al., 2011) proposed an animation method to generate direct 2D images without 3D simulations by considering the 2.5D velocity field. (Sato et al., 2012) also proposed a method that generated high-resolution 3D animations from low-resolution fluid simulations. Their database was constructed with only 2D fluid simulation results, and the low-resolution 3D simulation was performed based on the database, and the simulation results were converted to high-resolution animations.

As mentioned above, there is a lot of research on the simulation and the visualization of fire, which aim is to control the shape or to generate the images rapidly, and these methods are based on physical simulations. (Nguyen et al., 2002) also proposed a method for the physically-based modeling and the animation of fire. They used the incompressible Navier-Stokes equations and considered vaporized fuels and hot gaseous products. They also rendered the simulation results with a blackbody radiation model and represented the blue core in the chemical reaction zone. (Hamins and Bundy, 2005) simulated a candle flame with CFD (Computational Fluid Dynamics) model considering mass burning rate, candle regression rate, flame height, and heat flux obtained by their experiments. (Ogunedo and Okoro, 2017) also performed CFD flow simulation on a candle flame considering burning velocity, flame thickness, fuel flow rate, mass consumption rate, view factor, and heat flux.

However, they did not consider the combustion states. In fact, the flame color depends on the combustion states, which are divided into three kinds: complete combustion, incomplete combustion, and non-combustion. In addition, the combustion states depend on the physical property of the flammable materials. Then, (Mukai et al., 2019) proposed a method to simulate a candle flame by estimating the physical property of the material and to visualize the results by discriminating the combustion states. However, the result of the previous method showed a candle flame whose length was too short compared to that of a real candle. Therefore, this paper proposes a new method to simulate and visualize a candle flame by considering the temperature change in the environment because the temperature change affects the external force that elongates the candle flame.

2 CANDLE FLAME

2.1 Combustion States

Flame is divided into two types: premixed flame and diffusion flame. Premixed flame appears when the fuel gas and the air is uniformly premixed where the composition of the materials, the density, and the temperature are almost constant, while diffusion flame is generated as the fuel gas diffuses being mixed with the air when the combustion states are different and depend on the mixture ratio of the fuel gas and the air. The combustion states of the diffusion flame are divided into three types: complete combustion, incomplete combustion, and non-combustion. The color of the premixed flame is almost constant blue although the intensity is partly different, while the color of the diffusion flame is different according to the combustion states. The combustion states of a candle are shown in Fig. 1. Non-combustion and the wick of the candle are not fired so that the color is black, and the color of the incomplete combustion is almost orange or yellow, while the color of the complete combustion looks blue; however, it depends on the material and is decided by ion excitation.
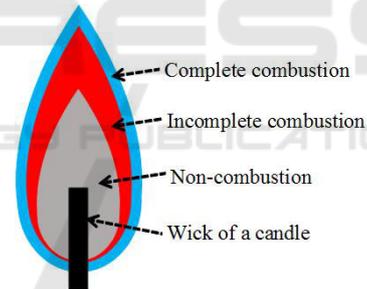

Figure 1: Combustion states of a candle flame.

2.2 Candle Property

The primary component of a candle is paraffin wax, which is the generic name of linear alkane and the chemical formula is C_nH_{2n+2} ($20 \leq n \leq 40$); however, the composition is not clear. Then, this paper supposes that a candle is composed of only Icosane, which is the simplest material of linear alkanes, and the formula is $C_{20}H_{42}$. Even if we assume that a candle is composed of only Icosane, there are a lot of unknown things that we have to estimate for the simulation. The chemical formula of complete combustion for Icosane is as follows.

$$2C_{20}H_{42} + 61O_2 \rightarrow 40CO_2 + 42H_2O \qquad (1)$$

On the other hand, the air is composed of 78% Nitrogen (N_2), 21% Oxygen (O_2), and 1% others. Then,

in Eq. (1), $61O_2$ is replaced with $290Air$ as follows since 290 Air includes $61(= 290 \times 0.21)$ Oxygen.

$$2C_{20}H_{42} + 290Air \rightarrow 40CO_2 + 42H_2O \qquad (2)$$

Then, the volume ratio of complete combustion for Icosane is 0.68 (=2/(2+290)) [$vol\%$] since the volume ratio equals the mole ratio. This means that if the volume ratio of the fuel gas is more than 0.68 [$vol\%$], the combustion state is incomplete because oxygen is not enough for the fuel gas.

On the other hand, if the volume ratio of the fuel gas is less than the threshold, the combustion state becomes non-combustion since the fuel gas is not enough. Then, the lower and the upper explosive limits of the combustion state is necessary for the simulation. However, the lower and the upper explosive limits of combustion states for Icosane are unknown. Then, they should be estimated from the simpler materials of linear alkane, which lower and upper explosive limits are shown in Table 1 (Nassimi et al., 2017).

Table 1: Lower and upper explosive limits of linear alkane.

				[$vol\%$]
Material	Formula	# of Carbon	Lower limit	Upper limit
Methane	C_1H_4	1	5.00	15.00
Ethane	C_2H_6	2	3.00	12.40
Propane	C_3H_8	3	2.10	9.50
Butane	C_4H_{10}	4	1.80	8.40
Pentane	C_5H_{12}	5	1.40	7.80
Hexane	C_6H_{14}	6	1.20	7.40
Heptane	C_7H_{16}	7	1.05	6.70
Octane	C_8H_{18}	8	0.92	6.50
Nonane	C_9H_{20}	9	0.80	6.00
Decane	$C_{10}H_{22}$	10	0.70	5.00

In addition, Fig. 2 shows the approximate curves of the lower and the upper explosive limits for linear alkanes and Icosane that carbon number is 20, and the lower and the upper explosive limits for Icosane are estimated as 0.02 [$vol\%$] and 1.35 [$vol\%$], respectively, from the extrapolation of the graph.

Then, the combustion states are summarized as shown in Table 2.

Table 2: Volume ratios and combustion states of Icosane.

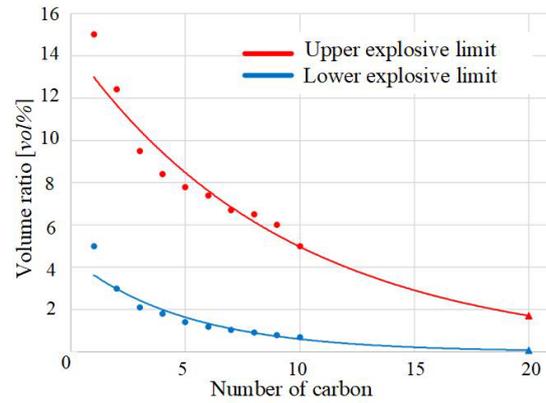| Volume ratio r [$vol\%$]	Combustion state	Burnable
r < 0.02	non-combustion	no
$0.02 \leq$ r < 0.68	complete	yes
$0.68 \leq$ r < 1.35	incomplete	yes
$1.35 \leq$ r	non-combustion	no

Figure 2: Approximate curves for the lower and the upper explosive limits.

2.3 Viscosity

The viscosity of a fuel gas changes depending on the material and the temperature. The viscosity of a material can be calculated with Sutherland's formula (CFDOnline, 2022), which is written in Eq. (3).

$$\mu = \frac{C_1 T^{\frac{3}{2}}}{T + C_2}, \qquad (3)$$

where, μ is the viscosity, T is the absolute temperature, C_1 and C_2 are the constants that depend on the material.

Then, if C_1 and C_2 are decided, the viscosity at the specific temperature can be calculated. However, the relationship between the viscosity and the temperature of Icosane is unknown. Then, it should be estimated with the simpler linear alkane, which viscosity for the temperature is shown in Table 3.

Table 3: Viscosity of the simpler linear alkane.

		[$\times 10^{-2} mPa \cdot s$]				
Material	# of C	Temperature [$°C$]				
		0	20	50	100	200
Methane	1	1.02	1.08	1.18	1.33	1.47
Ethane	2	0.86	0.92	1.01	1.15	1.43
Propane	3	0.75	0.80	0.88	1.01	1.25
Hexane	6	0.60	0.65	0.71	0.82	1.04

Fig. 3 shows the approximate curves estimated from Table 3, and the viscosity of Icosane, which carbon number is 20, can be estimated with Fig. 3.

Fig. 4 shows the relationship between the absolute temperature and the viscosity of Icosane, which is estimated by plotting all points at 20 on x axis in Fig. 3. With Fig. 4, we can estimate the viscosity from the absolute temperature, and calculate the constants of Sutherland's formula, C_1 and C_2, which are decided
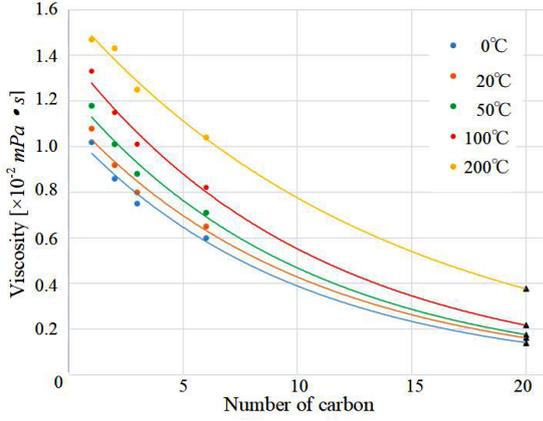
Figure 3: Approximate curves of the viscosity for simpler linear alkanes.

as 6.95×10^3 and 2.21×10^{10}, respectively. In Fig. 4, the horizontal axis is absolute temperature [K], which is calculated by adding 273.15 to Celsius degree [$°C$].
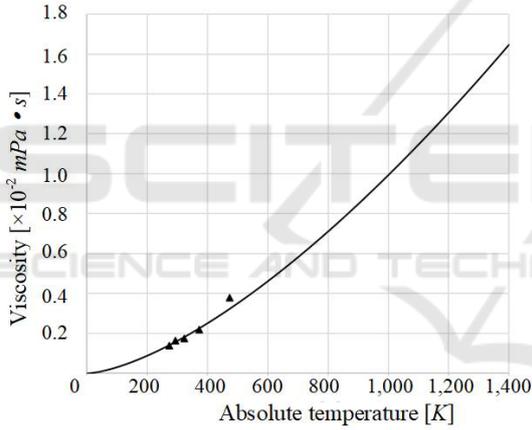

Figure 4: Relationship between the absolute temperature and the viscosity of Icosane.

The viscosity of Icosane is calculated from its temperature with Fig. 4. On the other hand, combustion states are decided by the volume ratio. Then, the relationship between the volume ratio and the temperature is necessary. Table 4 shows the relationship between combustion states and the limit temperature of a candle flame (ExplainThatStuff, 2022), where the volume ratios are added according to Table 2. In addition, the boiling point of Icosane is 615.85 [K], which volume ratio is 100 [$vol\%$]. Then, Fig. 5 is obtained by plotting all data, and shows the relationship between the volume ratio and the absolute temperature based on Table 4 and the boiling point of Icosane.

Table 4: Relationship between combustion states and limit temperatures.

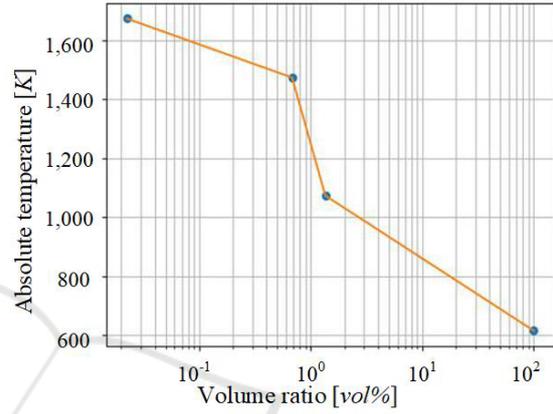| Combustion State	Temperature		Volume ratio [$vol\%$]
	Absolute [K]	Celsius [$°C$]	
Complete (max)	1,673.15	1,400	0.02
Complete (min) Incomplete (max)	1,473.15	1,200	0.68
Incomplete (min)	1,073.15	800	1.35

Figure 5: Relationship between volume ratio and absolute temperature of Icosane.

3 METHOD

3.1 Governing Equations

We employ SPH (Smoothed Particle Hydrodynamics) method for the simulation, and the governing equation is the Navier-Stokes equations written in Eq. (4).

$$\rho \frac{\partial \vec{u}}{\partial t} = -\nabla p + \eta \nabla^2 \vec{u} + \vec{f}, \qquad (4)$$

where, ρ is the density, $\vec{u}$ is the velocity, t is the time, p is the pressure, η is the viscosity coefficient, $\vec{f}$ is the external force.

Here, the density $\rho(\vec{x}_i)$ at the position of $\vec{x}_i$ is calculated as follows (Ertekin, 2015).

$$\rho(\vec{x}_i) = \sum_{j \neq i} m_j W_d(\vec{x}_j - \vec{x}_i)$$
$$= \sum_{j \neq i} m_j \frac{315}{64\pi r_e^9} (r_e^2 - |\vec{x}_j - \vec{x}_i|^2)^3, \qquad (5)$$

where, m_j is the mass of a particle j, W_d is the kernel function of the density, r_e is the radius of influence, and only $\vec{x}_j$ within r_e for $\vec{x}_i$ is counted.

Next, the pressure and the viscous terms at the position of $\vec{x}_i$ are calculated as follows (Ertekin, 2015).

$$
\begin{aligned}
-\nabla p &= -\sum_{j \neq i} m_j \frac{p_i + p_j}{2\rho_j} \nabla W_p(\vec{x}_j - \vec{x}_i) \\
&= -\sum_{j \neq i} m_j \frac{p_i + p_j}{2\rho_j} \frac{45}{\pi r_e^6}(r_e - |\vec{x}_j - \vec{x}_i|)^2 \frac{(\vec{x}_j - \vec{x}_i)}{|\vec{x}_j - \vec{x}_i|},
\end{aligned}
$$
(6)

$$
\begin{aligned}
\eta \nabla^2 \vec{u} &= \eta \sum_{j \neq i} m_j \frac{\vec{u}_j - \vec{u}_i}{\rho_j} \nabla^2 W_v(\vec{x}_j - \vec{x}_i) \\
&= \eta \sum_{j \neq i} m_j \frac{\vec{u}_j - \vec{u}_i}{\rho_j} \frac{45}{\pi r_e^6}(r_e - |\vec{x}_j - \vec{x}_i|),
\end{aligned}
$$
(7)

where, W_p and W_v are the kernel functions of the pressure and the viscosity, respectively.

The density $\rho(\vec{x}_i)$ at the position of $\vec{x}_i$ is calculated with Eq. (5), and suppose that the density of the flammable material that has only the fuel gas and no air is ρ_{max}. Then, the volume ratio of a particle i, which position is $\vec{x}_i$, is calculated as follows.

$$
\frac{\rho(\vec{x}_i)}{\rho_{max}}
$$
(8)

Then, the absolute temperature of a particle is estimated from the volume ratio with Fig. 5, and the viscosity (η) of the particle at the temperature is derived from Fig. 4.

At last, gravity, buoyancy, and environmental air pressure are considered as an external force. The buoyancy works for the fuel gas and the air in the combustion state. Then, the force that drives the buoyancy is calculated as follows.

$$
\vec{f}_b = (\rho_f - \rho_e)V_f \vec{g} + (\rho_a - \rho_e)V_a \vec{g},
$$
(9)

where, ρ_f, ρ_a, V_f, and V_a are the densities and the volumes of the fuel gas and the air in the combustion state, respectively. ρ_e is the density of the air that is placed in the environment, which has the room temperature (298.15 $[K]$ = 25 $[^\circ C]$), and $\vec{g}$ is the gravity.

The environmental air pressure is calculated with the following equation (Ueda and Fujishiro, 2014).

$$
\begin{aligned}
\vec{f}_e &= -\alpha \nabla p_e \\
&= -\alpha \sum_{j \neq i} m_j \frac{(p_e - p_i)}{\rho_j} \nabla W_p(\vec{x}_j - \vec{x}_i) \\
&= -\alpha \sum_{j \neq i} m_j \frac{(p_e - p_i)}{\rho_j} \frac{45}{\pi r_e^6}(r_e - |\vec{x}_j - \vec{x}_i|)^2 \frac{(\vec{x}_j - \vec{x}_i)}{|\vec{x}_j - \vec{x}_i|},
\end{aligned}
$$
(10)

$$
p_e = \rho_e R T_e,
$$
(11)

where, R and T_e are the coefficient of the ideal gas and the temperature of the environmental air, which is 298.15 $[K]$ (=25 $[^\circ C]$), respectively, and α is the adjustment factor for the simulation, and 0.01 is used in the simulation according to the experimental results.

Finally, the external force $\vec{f}$ in Eq. (4) becomes as follows.

$$
\vec{f} = (\rho_f V_f + \rho_a V_a)\vec{g} + \vec{f}_b + \vec{f}_e
$$
(12)

Here, the first term of the right-hand side is the gravity for the fuel gas and the air.

3.2 Temperature Change

In Eq. (11), p_e can be assumed as 1.0 $[atm]$ (= 0.1 $[MPa]$), and R is the coefficient of the ideal gas that has the value (8.3145 $[J/(mol \cdot K)]$). This means that the air density in the environment (ρ_e) can be calculated with the temperature in the environment (T_e), which depends on the distance from the wick of the candle. The candle flame is vertically long, while it is short in the horizontal direction. Then, the temperature change in the vertical direction from the wick of the candle is needed for the density calculation of the air. However, the particles of the air in the environment are not arranged, although the particles of the fuel gas are arranged considering the memory resources and the calculation time because a lot of particles are necessary for the simulation in the particle method. Then, the temperature of the air in the environment must be estimated.

The temperature in the position at 10 $[cm]$ (= 100 $[mm]$) in the vertical direction from the bottom of the candle flame was measured experimentally as 298.15 $[K]$ (= 25 $[^\circ C]$) that is the environmental temperature, while the temperature at the position in the horizontal direction was 298.15 $[K]$ (= 25 $[^\circ C]$) even if the position was near the candle flame. Then, we can estimate the air temperature in the vertical direction with interpolation between the wick of the candle and the position at 10 $[cm]$ from the wick. Here, the temperature of the wick of the candle was 1,262.44 $[K]$ in the simulation, although the average temperature of the incomplete state is 1.273.15 $[K]$ (= $(1,073.15 + 1,473.15)/2 [K]$).

In addition, a lot of particles are needed for the precise simulation, and in this paper, the size of the candle is 1/4 of that in the previous research (Mukai et al., 2019) for more precise simulation. Then, the interpolation equation of the temperature in the vertical direction becomes as follows.

$$T_e[K] = \begin{cases} 1,262.44[K] - \frac{1,262.44[K]-298.15[K]}{100[mm]/4}d \\ \qquad\qquad (0 \le d \le 25) \\ 298.15[K] \qquad (Otherwise), \end{cases}$$

(13)

where, d is the distance in the vertical direction from the wick of the candle, which unit is [mm].

4 SIMULATION AND RENDERING

The simulation algorithm is as follows.

< **Simulation Algorithm** >

1. Initialization: Set parameters and place particles around the wick of the candle.

2. Density calculation: Calculate the particle density with Eq. (5).

3. Pressure term calculation: Calculate the pressure term with Eq. (6).

4. Volume ratio calculation: Calculate the volume ratio with Eq. (8).

5. Temperature decision: Decide the particle temperature from the volume ratio with Fig. 5.

6. Viscosity decision: Decide the particle viscosity at the temperature with Fig. 4.

7. Viscosity term calculation: Calculate the viscosity term with Eq. (7).

8. Environmental temperature calculation: Estimate the environmental air temperature with Eq. (13).

9. External force term calculation: Calculate the external force with Eq. (12).

10. Particle position calculation: Calculate the acceleration, the velocity, and the position of a particle by solving Eq. (4).

11. Particle addition and removal: Add particles at the wick of the candle and remove particles that have burned out in the environment of the candle.

12. Rendering: Render the particles with the volume rendering method, which is described in the following.

13. Repeat the simulation from 2.

The simulation is performed with a particle method; however, the number of particles is not enough for the rendering. Then, the volume rendering method is employed to represent a candle flame by interpolating the density of each voxel in the grid. The rendering algorithm is as follows.

< **Rendering Algorithm** >

1. Grid space decision: Set the gird space that includes all particles, and expands it from the outermost positions by the radius of influence.

2. Voxel size: Set the voxel size as 1.1 times the particle diameter.

3. Density set: Set each voxel density. If there are some particles in a voxel, set the average as the density of the voxel. If there is no particle in a grid, set the density with IDW (Inverse Distance Weighting) interpolation (GISGeography, 2022), which is calculated with Eqs. (14) and (15).

The density is interpolated with the following equations.

$$\rho(\vec{x}) = \frac{\sum_{i=1}^{N} w_i(\vec{x})\rho(\vec{x}_i)}{\sum_{j=1}^{N} w_j(\vec{x})},$$

(14)

$$w_i(\vec{x}) = \frac{1}{d(\vec{x}, \vec{x}_i)^p},$$

(15)

$\rho(\vec{x})$ is the density of the voxel at the position of $\vec{x}$, $d(\vec{x}, \vec{x}_i)$ is the distance between the voxel at the position of $\vec{x}$ and the particle at the position of $\vec{x}_i$, and p is the order of the distance, which is 1 in this simulation. N is the number of particles that are within the radius of influence for the center of the voxel at the position of $\vec{x}$.

5 RESULTS

The simulation was performed with the PC, which specification is shown in Table 5. The grid size for the volume rendering changes dynamically according to the number of particles and the space the particles occupy. The maximum grid size was $65 \times 65 \times 65 = 274,625$.

Table 5: Specification of the PC used for the simulation.

OS	Windows 10 Education 64 bits
CPU	Intel Core i5-6400
Memory	8GB
GPU	NVIDIA GeForce GTX 1060 with 6 GB memory

Table 6 shows the comparison of the parameters between the previous simulation (Mukai et al., 2019) and the proposed one. The environmental air temperature was 298.15 [K] (= 25 [$°C$]).

The flame color in the incomplete combustion state is decided with the linear interpolation according to Table 7, which shows the color of the blackbody

41

Table 6: Comparison of the simulation parameters.

Parameters	Previous	Proposed
Particle radius	125 [μm]	31.25 [μm]
Grid size	125 [μm]	37.50 [μm]
Time steps	800	1,000
Real time per step	1.25 [μs]	0.3125 [μs]

radiation (MitchellCharity, 2022). The temperature in the incomplete combustion state is between 1,073.15 [K] and 1,473.15 [K] according to Table 4.

Table 7: Candle flame color.

Temperature [K]	R	G	B
1,000	255	56	0
1,200	255	83	0
1,400	255	101	0
1,600	255	115	0
1,673	255	120	0

On the other hand, the flame color in the complete combustion state is decided by ion excitation, and there is no reference on it. Then, the color is picked from the photograph of a real candle and decided as (94, 232, 255) in (R, G, B) color space.

Fig. 6 shows the simulation results of a candle flame. The left side images are the results in the previous simulation (Mukai et al., 2019), while the right side images are the results in the proposed method. In the simulation, spontaneous combustion at the wick of the candle is supposed. In Fig. 6, the size of this simulation is 1/4 of the previous one so the images on the right side are smaller than those on the left side. The shape of the flame on the right side is, however, thinner than that on the left side and the flame is vertically elongated because the proposed method calculates the external force $\vec{f}_e$ in Eq. (10) by considering the temperature change in the environment with the Eq. (13).

In addition, Fig. 7 shows the comparison of the simulation result with a real candle flame. Fig. 7 (a) shows the simulation results of the proposed method at the time step of 1,000, while Fig. 7 (b) shows a real candle flame. The shape of the flame in (a) is similar to that in (b), and the color at the bottom of the flame is orange in both (a) and (b); however, the color at the tip of the flame in (a) is orange, while that in (b) is yellow, which means the temperature in the simulation is lower than that in the real candle. In addition, the color at the center of the flame in (a) is yellow, which means that the temperature of the center is higher than that of the surroundings in the simulation result (a), while the temperature of the center is lower than that of the surroundings in the real candle.

(a) 200 steps

(b) 400 steps

(c) 800 steps
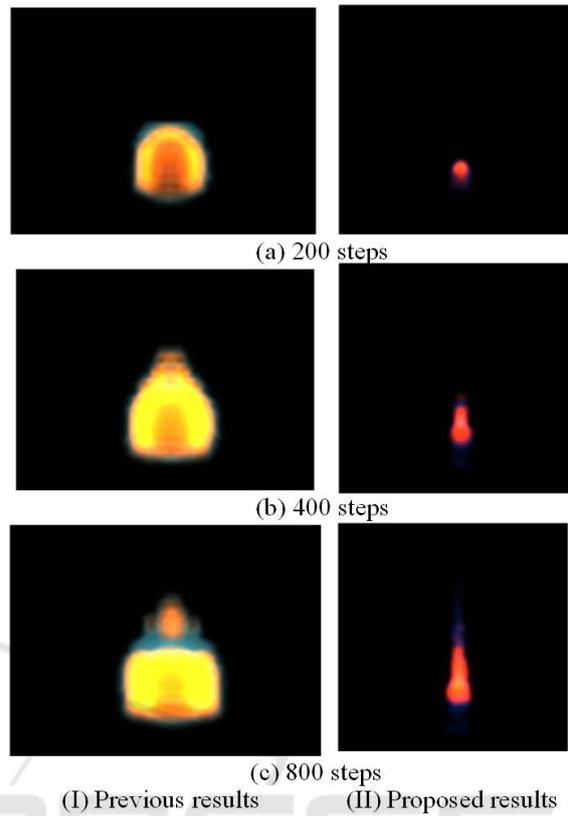
(I) Previous results (II) Proposed results

Figure 6: Comparison of the results between the previous and the proposed methods.

In real combustion, oxygen in the center of the candle is less than that in the surroundings, and the state is incomplete combustion so that the temperature in the center is lower than that in the surroundings. On the other hand, the surroundings of the flame have plenty of oxygen so that the state is the complete combustion, and the temperature is high although the blue color that indicates the complete combustion is not seen in the real candle because the color of the background is black, while the tip and the bottom of the flame in (a) have slight blue color that indicates the complete combustion.
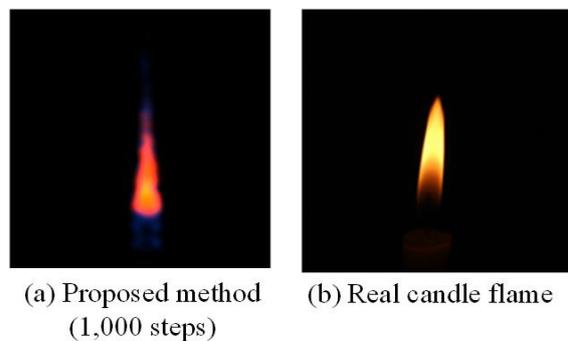

(a) Proposed method (b) Real candle flame
(1,000 steps)

Figure 7: Comparison with a real candle flame.

6 CONCLUSIONS

Fire is very familiar to human beings and there are many scenes using fire in movies, games, and so on. Then, a lot of studies have been performed to simulate and visualize fire. Some of them are on controlling the shape by users, and others are methods to represent realistic fire in real time. However, most previous works treated the fire only in the incomplete combustion state without the complete combustion. In addition, the most familiar fire is a candle flame; however, the component of a candle is unknown although the material is paraffin.

Then, we proposed a method to simulate and visualize the candle flame with a particle method by considering the three states of combustion: complete combustion, incomplete combustion, and non-combustion in the previous method. We also assumed that the candle is composed of only one material of "Icosane", and estimated the viscosity that depends on the absolute temperature, which also depends on the volume ratio of the fuel gas. However, the flame shape of the simulation result in the previous method was not similar to that of a real candle. Then, in this paper, we have proposed a new method to simulate the candle flame by interpolating the environmental air temperature, which affects the density of the environmental air that changes the external force.

As the comparison of the simulation results between the previous and the proposed methods, the shape of the flame in the proposed method was thinner than that of the previous method and was elongated vertically. It was similar to the flame of the real candle, and the overall color was also similar.

However, the color of the surroundings in the simulation result was orange, while the color of the area in the real candle flame was yellow. In addition, the temperature at the center of the simulated flame was higher than that in the surroundings, while the temperature at the surroundings was higher than that at the center in the real candle flame. Then, we plan to investigate the reasons for these differences and consider the more precise simulation method in the future.

REFERENCES

Bangalore, A. and House, D. H. (2012). A technique for art direction of physically based fire simulation. In *The 8th Annual Symposium on Computational Aesthetics in Graphics, Visualization, and Imaging*, pages 45–54.

CFDOnline (Referenced in March 2022). Sutherland's law. https://www.cfd-online.com/Wiki/Sutherland's_law.

Cha, M., Lee, J., Choi, B., Lee, H., and Han, S. (2009). A data-driven visual simulation of fire phenomena. In *ACM SIGGRAPH Posters*, page Article No.74.

Ertekin, B. (2015). *Fluid Simulation using Smoothed Particle Hydrodynamics*. Bournemouth University.

ExplainThatStuff (Referenced in March 2022). The science of candles. https://www.explainthatstuff.com/candles.html.

GISGeography (Referenced in March 2022). Inverse distance weighting (IDW) interpolation. https://gisgeography.com/inverse-distance-weighting-idw-interpolation.

Guay, M., Colin, F., , and Egli, R. (2011). Screen space animation of fire. In *ACM SIGGRAPH Asia Sketches*, page Article No.10.

Hamins, A. and Bundy, M. (2005). Characterization of candle flames. *Journal of Fire Protection Engineering*, 15:265–285.

Hladký, J. (2018). Fire simulation in 3d computer animation with turbulence dynamics including fire separation and profile modeling. *International Journal of Networking and Computing*, 8(2):186–204.

Horvath, C. and Geiger, W. (2009). Directable, hight-resolution simulation of fire on the gpu. *ACM Transactions on Graphics*, 28(3):Article No.41.

Louchez, F. B., Leblond, M., and Rousselle, F. (2006). Enhanced illumination of reconstructed dynamic environments using a real-time flame model. In *AFRIGRAPHAFRIGRAPH*, pages 31–40.

MitchellCharity (Referenced in March 2022). What color is a blackbody? - some pixel rgb values. http://www.vendian.org/mncharity/dir3/blackbody.

Mukai, N., Akasaka, S., and Chang, Y. (2019). Candle flame simulation considering combustion states. In *IIEEJ International Conferences on Image Electronics and Visual Computing*, page 4.

Nassimi, A. M., Jafari, M., Farrokhpour, H., and Keshavarz, M. H. (2017). Constants of explosive limits. *Chemical Engineering Science*, 173:384–389.

Nguyen, D. Q., Fedkiw, R., and Jensen, H. W. (2002). Physically based modeling and animation of fire. *ACM Transactions on Graphics*, 21(3):721–728.

Ogunedo, M. B. and Okoro, V. I. (2017). Cfd simulation of a candle flame propagation. *Elixir Journal of Mechanical Engineering*, 108:47813–47817.

Sato, S., Mizutani, K., Dobashi, Y., Nishita, T., and Yamamoto, T. (2017). Feedback control of fire simulation based on computational fluid dynamics. *Computer Animation and Virtual Worlds*, 28(3-4 e1766).

Sato, S., Morita, T., Dobashi, Y., and Yamamoto, T. (2012). A data-driven approach for synthesizing high-resolution animation of fire. In *The Digital Production Symposium*, pages 37–42.

Ueda, K. and Fujishiro, I. (2014). Splashing liquids with ambient gas pressure. In *ACM SIGGRAPH Asia Technical Briefs*, page Article No.6.

Wei, X., Li, W., Mueller, K., and Kaufman, A. (2002). Simulating fire with texture splats. In *The conference on Visualization*, pages 227–235.